Fusion-Fission versus Quasifission: Effect of Nuclear Orientation

D. J. Hinde, M. Dasgupta, J. R. Leigh, J. P. Lestone, J. C. Mein, C. R. Morton, J. O. Newton, and H. Timmers
Department of Nuclear Physics, Research School of Physical Sciences and Engineering, Australian National University, Canberra, ACT 0200, Australia
(Received 28 October 1994)

Fission fragment angular distributions and cross sections have been measured for the reaction of $^{16}O + ^{238}U$ at energies around the Coulomb barrier. Full momentum transfer events were selected using the folding angle technique. The fission fragment anisotropies rise rapidly as the beam energy decreases through the barrier region. This is interpreted as showing that collisions with the tips of the deformed target nucleus lead to quasifission, collisions with the sides to fusion-fission.

PACS numbers: 25.70.Jj

The fusion of two heavy nuclei is a very basic phenomenon in the study of nuclear physics; yet there are dynamical aspects which are not fully understood. For heavy systems, with large Coulomb repulsion, there is a dramatic reduction of the true fusion probability, which is a severe obstacle to the formation of superheavy elements [1]. Because of the high probability of fission, obtaining detailed information about this effect through studying those nuclei which survive fission is a very difficult task. However, the angular distribution of the fission fragments can in principle give useful information about the reaction preceding the scission event. The angular distribution is characterized by the anisotropy, defined as the ratio of yields at 0° or 180° to that at 90° to the beam axis. This is denoted by $W(0°)/W(90°)$ or $W(180°)/W(90°)$.

In the case of fission following fusion, with complete equilibration of all degrees of freedom of the compound nucleus, the anisotropy is determined by the mean square angular momentum $\langle J^2 \rangle$ of the compound nucleus and by the effective moment of inertia and temperature of the nucleus, calculated in the transition state model [2] at the saddle point. The predictions of fusion models have compared well [3,4] with $\langle J^2 \rangle$ values extracted from measured anisotropies for light projectiles ($Z \leq 8$).

For heavy compound nuclei ($A > 230$) formed with heavy projectiles, measured anisotropies [5] substantially exceed calculated values. It is accepted that fissionlike events (quasifission) occur from systems which, due to the large Coulomb repulsion, never reached the compact equilibrium configuration. This results in a large anisotropy.

For reactions in the transition between these two regimes (^{16}O or ^{19}F on ^{232}Th or ^{238}U targets) the anisotropy increases as the bombarding energy decreases near the fusion barrier. Earlier data [6,7] included fission following transfer, which clouded the picture. More recent data [8] eliminate this contribution, and still show an increase. No satisfactory explanation for this energy dependence has been given.

New high precision data presented in this Letter have inspired a simple and intuitive explanation for this phenomenon. It should be applicable to all reactions involving deformed nuclei where quasifission and fusion-fission are in competition, and has important implications for understanding and predicting production cross sections for superheavy elements.

The experiment was performed at the 14UD tandem accelerator of the Australian National University. A target of $^{nat}UF_4$ of $\simeq 220\ \mu g\,cm^{-2}$ deposited on a $\simeq 15\ \mu g\,cm^{-2}$ C foil was bombarded with ^{16}O beams of $76 \leq E_{lab} \leq 104$ MeV. Fission fragments were detected in two position sensitive multiwire proportional chambers (MWPCs), each with active area $28 \times 36\ cm^2$, centered at 45° and −135°, and located 18 cm from the target. Two monitor detectors were placed at angles of 22° above and below the beam axis. The position information from the MWPCs was transformed to give the scattering angles Θ_{lab} and azimuthal angles Φ_{lab}. For a cut of 70° in Φ_{lab}, slices of 5° in Θ_{lab} were made in the back angle detector, and the folding angle spectrum for each slice was projected. These showed a main peak consistent with fission following full momentum transfer (FMT), and a subsidiary peak corresponding to fission following transfer or incomplete fusion, as illustrated in Fig. 1(a). At near-barrier energies, the projectile remnant recoils to backward angles. Thus the folding angle for fission following transfer is smaller than that for FMT, and the kinematics causes the fission yield to decrease at angles closer to the beam axis. This is in contrast with the situation if slices in Θ_{lab} are made at forward angles, in which case the relative yield would increase. The method used thus minimizes the contribution from fission following transfer at near-barrier energies. Cross sections were normalized to Rutherford scattering by performing a calibration run at a sub-barrier energy in which elastically scattered ^{28}Si projectiles were detected.

Angular distributions of the FMT component in its c.m. frame were generated at each energy. These were fitted using distributions calculated [8] with the transition state model, in order to obtain the total fission cross section and the anisotropy $W(180°)/W(90°)$. An example is shown in Fig. 1(b). Also shown is the angular distribution for all fissions; since the kinematic transformation assumes

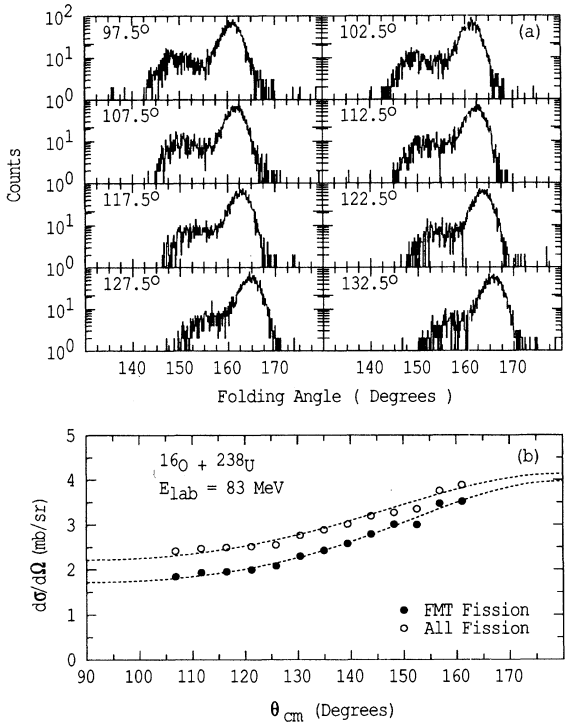

FIG. 1. (a) shows the fission folding angle distributions for 83 MeV $^{16}O + ^{238}U$ at the indicated mean laboratory angles. Extraction of the full momentum transfer component results in the angular distribution shown in (b). Also shown is the distribution for all fissions. The fitted angular distributions from which the anisotropies and cross sections were determined are shown by the dashed lines.

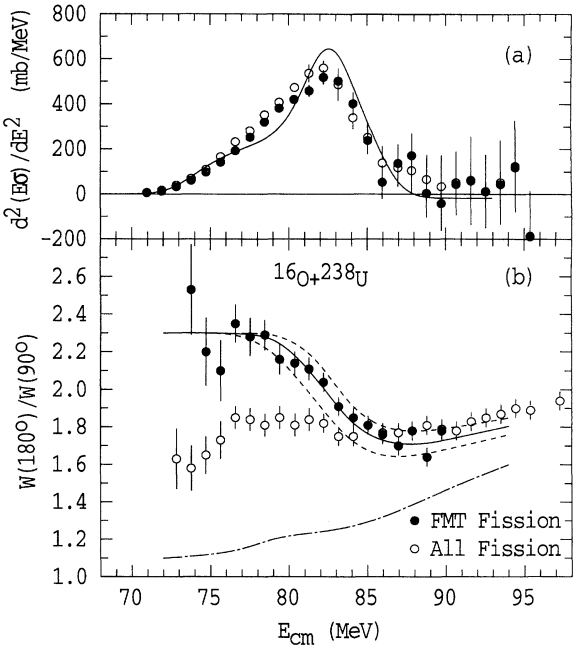

FIG. 2. (a) shows the curvature of the FMT fission excitation function (full points) and that for all fissions (hollow points). The former is proportional to the fusion barrier distribution. The fission anisotropies are shown in (b) with the same symbols. The expected anisotropy based on the transition state model is given by the dot-dashed line, while the model described in the text results in the full and dashed lines.

FMT, these fits do not result in physically meaningful cross sections or anisotropies. At energies above $E_{c.m.} = 90$ MeV, it is not possible to clearly separate the two fission components since the recoil direction of the projectile remnant moves to more forward angles, and the momentum transfer in the beam direction is no longer larger than that for complete fusion. It was found that the ratio of fission cross sections extracted for FMT fission to those for all fissions saturated at 0.91 before $E_{c.m.} = 90$ MeV, so at higher energies the former cross sections were estimated by scaling the latter by 0.91. As will be seen, this is already above the most interesting energy region, and so does not affect the conclusions.

This analysis procedure resulted in a set of fission cross sections and anisotropies for FMT fission, and for all fissions extracted using the kinematics for FMT fission. Since the evaporation residue yield is negligible for this reaction, the FMT fission cross sections constitute the fusion cross sections σ_{fus}.

The curvature of the function $E_{c.m.}\sigma_{fus}$ with respect to energy represents the distribution of fusion barriers [9]. This was determined from the measured $E_{c.m.}\sigma_{fus}$ values using a point-difference formula [10] with an energy step of 1.87 MeV. It is shown in Fig. 2(a) by the solid points.

Because of the high statistics and large solid angle of the detectors, the fusion barrier distribution is very well defined, and the assumption that random uncertainties are not less than 0.5% appears to be conservative, based on the lack of scatter of the data points at the higher energies. The "barrier distribution" extracted from the fits to all fissions is also indicated by hollow points. Since this is derived from cross sections which include some transfer-induced fission using inappropriate kinematics, it is interesting that the true distribution is reproduced with surprisingly little distortion.

The shape of the fusion barrier distribution is very similar to that previously determined [10,11] for the reaction $^{16}O + ^{154}Sm$, and is characteristic of a prolate deformed nucleus. This is supported by a calculation using the code CCMOD [12], with tabulated [13] ^{238}U deformation parameters $\beta_2 = 0.275$ and $\beta_4 = 0.05$, which gives a reasonable reproduction of the data, as shown in Fig. 2(a).

The fission fragment anisotropies are shown in Fig. 2(b). As the bombarding energy decreases through the barrier region, the FMT anisotropies rise rapidly, then ultimately seem to saturate. This correlation with the barrier distribution is very striking, and immediately suggests a relationship between the anisotropy and the height of the fusion barrier encountered in a given collision.

Considering the collision classically, the higher barriers correspond to contact of the projectile with the flattened side of the prolate target, resulting initially in a compact dinuclear system. Conversely, the lower barriers correspond to contact with the tip, giving an elongated dinuclear system. Intuitively, it seems reasonable that the former configuration would be more likely to result in fusion-fission, and the latter in quasifission. These limiting configurations are illustrated in Fig. 3. Once inside the respective fusion barriers, and the radial motion is rapidly damped, the nuclear system will start to evolve over the potential energy surface of the combined system. Important features of the potential energy surface (PES) for this system are sketched in Fig. 3. The axes represent the mass asymmetry, defined as $\alpha = (M_H - M_L)/(M_H + M_L)$, and the separation D of the centers of mass of the two incipient fragments, defined in units of the radius of the spherical configuration (R_0), as in Ref. [14]. The equilibrium configuration, which should be reached for fusion-fission to occur, is close to the line corresponding to a sphere. The ridge line represents the locus of configurations of the conditional (α-fixed) saddle points. If D is beyond the ridge line, the PES forces the system to scission. The curve in Fig. 3 was estimated by extrapolation from the results of Ref. [14] for lighter nuclei. For fissile systems, with the model used, it proved possible to define the ridge line only at large and small α (solid line), since at intermediate values the field of the smaller fragment deforms the larger one over its own saddle point

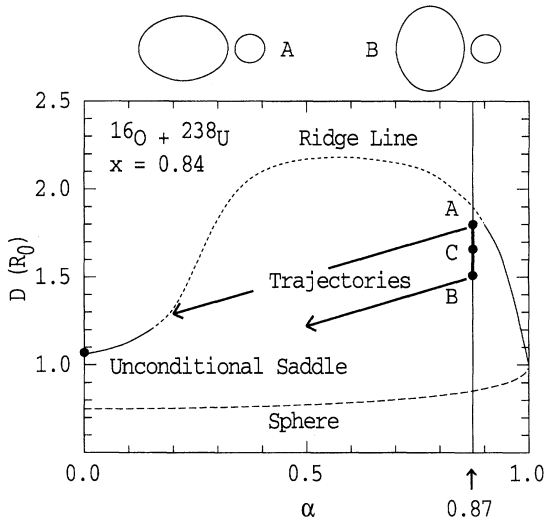

FIG. 3. The fusion barrier configurations for $^{16}O + ^{238}U$ corresponding to collision with the tips (A) and sides (B) of the deformed ^{238}U. These points are indicated on the potential energy surface, as a function of the center of mass separation D and the mass asymmetry α. The spherical configuration and the estimated position of the conditional fission saddle ridge line are shown. Possible trajectories are sketched from injection points A and B, leading to quasifission and fusion-fission, respectively.

[14]. Since the nuclei still undergo symmetric fission, nature must provide a ridge line; however, its location is not yet well defined, and may be at considerably smaller values of D than indicated by the dashed line.

Whether the system evolves in the direction of $\alpha = 0.0$ or $\alpha = 1.0$ is of crucial importance in determining the outcome of the reaction and is expected [15] to be determined by the PES. In particular, the Businaro-Gallone critical asymmetry α_{BG} defines the point on the ridge line where the potential energy is at its maximum. For this system, $\alpha_{BG} \sim 0.90$, while the injection point is at $\alpha = 0.87$ (before N/Z equilibration). Experimental measurements of anisotropies at energies above the barrier region have been used [3,15] as evidence to show that for this reaction the system does move towards $\alpha = 0.0$. Thus we can picture the projectile "sucking up" matter from the target. The trajectories over the PES will depend in detail on the PES and the inertia and viscosity tensors. However, experimental evidence [16] shows that the mass-asymmetry degree of freedom equilibrates more rapidly than the elongation does. Thus, qualitatively, the trajectory leading from the most compact injection point (B) may be as indicated on Fig. 3 by the arrow, resulting in fusion-fission. Moving the injection point out to larger D should cause the system to cross the ridge line at finite asymmetry, as illustrated, resulting in quasifission. The combined effect of the larger effective moment of inertia compared to that of the unconditional saddle point at $\alpha = 0.0$, and the fact that K equilibration [17] may not occur, will result in a large anisotropy.

A simple empirical geometrical model to test this picture has been developed. It is assumed that collisions with the tips of the target nuclei result in quasifission only; the data at the lowest energies then show that quasifission has an anisotropy of 2.3, which is used at all energies. The anisotropy for fusion-fission is taken from the transition state model, and is shown by the dot-dashed curve in Fig. 2(b). A sharp transition between quasifission and fusion-fission is assumed to occur at a critical fusion barrier radius. The average anisotropy was determined by weighting the anisotropies with the cross sections resulting from passage over fusion barriers with radii, respectively greater and smaller than the critical radius. Taking a critical radius of 12.4 fm (point C in Fig. 3), corresponding to an angle between the beam axis and the target nucleus symmetry axis of 35°, the resulting average anisotropies are as shown by the solid curve in Fig. 2(b). They follow the trend of the data very well, supporting the hypothesis. The effects of a $\pm 5°$ change in angle are indicated by the dashed lines.

The experimental feature observed is well defined and distinctive, and describing it should be a challenging test of the reliability of transport models of fusion and fission. It would be of interest to compare calculations with detailed measurements from other projectile and target

combinations, and to look for any variation of fission mass distribution with energy. Such measurements are planned.

In all reactions where fusion-fission and quasifission are competing reaction modes, and a range of fusion barrier radii are involved, the effect described here should be present. Experiments in which fusion reactions are used to form superheavy nuclei could be significantly affected. The results presented here indicate that, in attempting to form such very fissile nuclei near their equilibrium deformation, only reactions associated with passage over the highest fusion barriers can result in the compact shapes which lead to the survival of evaporation residues. The use of targets and projectiles with the largest possible deformations may thus give the most favorable result. Clearly more experimental data and more sophisticated model calculations need to be available before the full implications for superheavy element production can be assessed.

In conclusion, new precise measurements have been made of the cross sections and anisotropies of fission fragments following full momentum transfer for the reaction $^{16}O + ^{238}U$. The former allow extraction of the fusion barrier distribution, which shows that ^{238}U behaves in fusion as a prolate deformed nucleus, as expected. The anisotropies rise rapidly as the beam energy drops through the fusion barrier region, then saturate. The correlation between barrier energy and radius leads to the conclusion that in this reaction collisions with the tips of the deformed target nuclei lead to quasifission, while collisions with the sides result in fusion-fission.

[1] Yu. Ts. Oganessian, in Proceedings of the Second International Conference on Dynamical Aspects of Nuclear Fission (JINR Report No. E7-94-19, 1994), p. 11.
[2] R. Freifelder, M. Prakash, and J. M. Alexander, Phys. Rep. **133**, 315 (1986), and references therein.
[3] A. Saxena *et al.*, Phys. Rev. C **47**, 403 (1993), and references therein.
[4] D. J. Hinde *et al.*, in Proceedings of the Fifth International Conference on Nucleus-Nucleus Collisions, Taormina, Italy, 1994 [Nucl. Phys. **A** (to be published)].
[5] B. B. Back *et al.*, Phys. Rev. C **32**, 195 (1985).
[6] T. Murakami *et al.*, Phys. Rev. C **34**, 1353 (1986).
[7] H. Zhang *et al.*, Phys. Rev. C **42**, 1086 (1990).
[8] H. Zhang *et al.*, Phys. Rev. C **49**, 926 (1994).
[9] N. Rowley, G. R. Satchler, and P. H. Stelson, Phys. Lett. B **254**, 25 (1991).
[10] J. X. Wei *et al.*, Phys. Rev. Lett. **67**, 3368 (1991).
[11] J. R. Leigh *et al.*, Phys. Rev. C **47**, R437 (1993).
[12] M. Dasgupta *et al.*, Nucl. Phys. **A539**, 351 (1992).
[13] E. N. Shurshikov, Nucl. Data Sheets **53**, 601 (1988).
[14] K. T. R. Davies and A. J. Sierk, Phys. Rev. C **31**, 915 (1985).
[15] V. S. Ramamurthy *et al.*, Phys. Rev. Lett. **65**, 25 (1990).
[16] J. Tōke *et al.*, Nucl. Phys. **A440**, 327 (1985).
[17] V. S. Ramamurthy and S. S. Kapoor, Phys. Rev. Lett. **54**, 1234 (1985).